# Soft Matter

# Dual stimuli-responsive coating designed through layer-by-layer assembly of

# PAA-b-PNIPAM block copolymers for the control of protein adsorption

A. Osypova [a, b, c], D. Magnin [a], P. Sibret [d], A. Aqil [d], C. Jérôme [d], C. Dupont-Gillain [a],

C.-M. Pradier [b, c], S. Demoustier-Champagne [a, *], J. Landoulsi [b, c,*]

[a] *Institute of Condensed Matter and Nanosciences, Bio & Soft Matter, Université catholique de Louvain, Croix du Sud 1 (L7.04.01), 1348, Louvain-la-Neuve, Belgium*

[b] *Sorbonne Universités, UPMC Univ Paris 06, F-75005, Paris, France*

[c] *CNRS, UMR 7197, Laboratoire de Réactivité de Surface, F-75005, Paris, France*

[d] *Center for Education and Research on Macromolecules (CERM), Chemistry Department, University of Liege (ULg), Sart-Tilman, B6a, 4000 Liège, Belgium*

[*] corresponding authors : sophie.demoustier@uclouvain.be, jessem.landoulsi@upmc.fr

**Soft Matter Accepted Manuscript**

1

## Abstract

In this paper, we describe the successful construction, characteristics and interaction with proteins of stimuli-responsive thin nanostructured films prepared by layer-by-layer (LbL) sequential assembly of PNIPAM-containing polyelectrolytes and PAH. PAA-b-PNIPAM block copolymers were synthesized in order to benefit from (i) the ionizable properties of PAA, to be involved in the LbL assembly, and (ii) the sensitivity of PNIPAM to temperature stimulus. The impact of parameters related to the structure and size of the macromolecules (their molecular weight and the relative degree of polymerization of PAA and PNIPAM), and the interaction with proteins under physico-chemical stimuli, such as pH and temperature, are carefully investigated. The incorporation of PAA-b-PNIPAM into multilayered films is shown to be successful whatever the block copolymer used, resulting in slightly thicker films than the corresponding $(PAA/PAH)_n$ film. Importantly, the protein adsorption studies demonstrate that it is possible to alter the adsorption behavior of proteins on $(PAA-b-PNIPAM/PAH)_n$ surfaces by varying the temperature and/or the pH of the medium, which seems to be intimately related to two key factors: (i) the ability of PNIPAM units to undergo conformational changes and (ii) the structural changes of the film made of weak polyelectrolytes. The simplicity of construction of these PNIPAM block copolymer-based LbL coatings on a large range of substrates, combined with their highly tunable features, make them ideal candidates to be employed for various biomedical applications requiring the control of protein adsorption.

## 1. Introduction

Layer-by-layer (LbL) sequential assembly of polyelectrolytes is a powerful yet straightforward technique for the elaboration of nanostructured films with tailored properties and functions [1]. In particular, the use of this technique has attracted a growing interest for the elaboration of interfaces between materials and biological systems, which may control the adsorption behavior of proteins and their subsequent interaction with cells [2, 3]. In addition to the high versatility of the technique, the major advantages of LbL, in this context, lie into two important aspects: (i) the ability of polyelectrolyte multilayers (PEM) to adhere on wide ranges of substrates with diverse natures and shapes, and (ii) the possibility to achieve specific surface features that response to changes in the medium, such as pH, temperature and ionic strength, i.e. factors influencing the adsorption of proteins at solid/liquid interface. pH stimulus has been extensively studied for LbL films containing weak polyelectrolytes, showing noticeable changes in the film structure (swelling/deswelling) [4-6] and the resulting capacity to host/release biomolecules [7]. By contrast, temperature stimulus requires the incorporation of thermo-responsive, mostly non ionizable, polymer units. Poly(N-isopropylacrylamide) (PNIPAM) is one of the most studied polymers which is known for its high thermo-sensitivity either as free macromolecules in solution [8] or immobilized on solid surfaces [9, 10]. Owing to its chemical structure, PNIPAM possesses a lower critical solution temperature (LCST) of ~32 °C. Below this temperature, the polymer exhibits hydrophilic moieties and can thus be used for the design of protein repellent surfaces[11, 12]. By contrast, above the LCST, PNIPAM undergoes entropy-governed conformational changes and forms hydrophobic globules, which may attract biomacromolecules.

One relevant way to incorporate NIPAM units in LbL coatings has been achieved by the synthesis of polyelectrolyte-b-PNIPAM block copolymers [13]. Actually, the use of block

copolymers as constituents in LbL films has been explored during the last decades, owing to the progresses made in polymer synthesis, especially controlled radical polymerization techniques [14]. In aqueous media, i.e. in conditions used for LbL assembly, block copolymers may self-assemble to form micelles composed of a hydrophobic core and water-soluble hydrophilic coronae. The so called "block copolymer micelles" (BCM) may exhibit high sensitivity to environmental stimuli when adsorbed on solid surface, such as reversible dissolution of micellar cores [15].

PNIPAM-containing block copolymers may also form thermo-responsive micelles. For instance, PMMA-b-PNIPAM, block copolymers self-assemble into core-shell micelles with hydrophobic PMMA cores and hydrophilic PNIPAM shells. At temperature above the LCST, PNIPAM hydrophobic globules are forming and aggregation occurs as the chains tend to avoid contact with water [16]. Similar behavior has been reported for PNIPAM-b-PS [17] and PNIPAM-b-PDLL [18]. Erel et al. have reported the micellization of PDMA-b-PNIPAM block copolymers and revealed the existence of three types of micelles, including micelles with a PNIPAM corona and a pH-responsive core composed of the weak polyelectrolyte (PDMA) [19].

Recently, Sukhishvili et al. have explored the functionality of PNIPAM-containing BCMs to elaborate LbL films using diverse systems such as (PVPON-*b*-PNIPAM), [20] (PDMA-b-PNIPAM) [21] and (PDEA-b-PNIPAM) [22]. To this end, the authors have dissolved block copolymers in aqueous solutions in conditions that insure a micellar form of the macromolecules. Results evidenced the ability of BCMs to preserve their state when incorporated in the LbL films and to exhibit stimuli-responsive behavior [21].

In most cases, the latter properties have been examined in terms of morphological features of the LbL film, which is influenced by the size of micelles and their degree of swelling. However, to the best of our knowledge, subsequent interactions with proteins under stimuli have never been

4

explored for such systems. Moreover, the incorporation of polyelectrolyte-b-PNIPAM in LbL assembly using weak polyelectrolyte blocks remains poorly documented [19]. These macromolecules are, yet, potential candidates to explore dual stimuli, namely pH and temperature. Using a weak polyelectrolyte as one segment of the diblock is a major advantage as its swelling behavior may be explored to create multilayers in which thermo-responsive units are not hindered by the surrounding polymer chains, thus preserving partial mobility under stimuli.

In this paper, we investigate the ability of a variety of PAA-b-PNIPAM block copolymers, which differ by their block lengths, to be assembled in LbL films at room temperature with PAH as polycation. The combination of pH-responsive PAA and thermo-responsive PNIPAM, in a block copolymer, leads to a system that may respond to both pH and temperature. This effect has been proven for PAA-b-PNIPAM block copolymers in aqueous medium [23]. In the present study, we explore the strategy of including a dual sensitivity to temperature and pH in LbL films and examine its impact on the interaction with proteins. For this purpose, the build-up of (PAH/PAA-b-PNIPAM)$_n$ multilayers was monitored *in situ* by quartz crystal microbalance with dissipation monitoring (QCM-D) and *ex situ* by ellipsometry. The adsorption behavior of proteins was then examined both on (PAH/PAA-b-PNIPAM)$_n$ and (PAH/PAA)$_n$ for sake of comparison, while varying either the temperature or the pH of protein solution.

## 2. Experimental section

### 2.1. Materials

*N*-isopropylacrylamide (Aldrich; 97%) was recrystallized twice from benzene/hexane 3:2 (v/v) and dried under vacuum prior to use. 2,2'-Azobis(isobutyronitrile) (AIBN, Fluka) was recrystallized from methanol. Acrylic acid (Aldrich) was purified by distillation under reduced pressure. 2-dodecylsulfanylthiocarbonylsulfanyl-2-methyl propionic acid (DMP),

dimethylformamide (DMF) and 2,2-azobis(4-methoxy-2,4-dimethylvaleronitrile) (V70) were used as received. Poly(allylamine hydrochloride) (PAH, Mw = 15 kDa), poly(acrylic acid sodium salt) (PAA, Mw = 5.1 kDa and Mw = 15 kDa), albumin from chicken egg (ovalbumin Mw = 46 kDa), sodium acetate, acetic acid, sodium hydroxide were purchased from Sigma-Aldrich (Belgium). Ethanol 96% was purchased from VWR (Belgium). Ultrapure water (MilliQ, Millipore, France) was used for the preparation of all buffer solutions.

### 2.2. Synthesis of PAA-b-PNIPAM block copolymers

Block copolymers F10 (PAA 5.70 kDa – PNIPAM 2.1 kDa), F11 (PAA 5.70 kDa – PNIPAM 11 kDa) and F22 (PAA 13.4 kDa – PNIPAM 15.4 kDa) were synthesized according to previously reported work [24]. Below, the synthesis conditions are detailed for the F10 copolymer, the monomers composition was simply adjusted for the two other F11 and F22 copolymers.

*i. Synthesis of PAA first block (PAA-CTA).* 0.012 g of azo-bis-isobutyronitrile ($7.31 \times 10^{-5}$ mol), 1.09 g of DMP ($3 \times 10^{-3}$ mol), 20 mL of AA ($2.91 \times 10^{-1}$ mol) and 20 mL of DMF were mixed together in a 250 mL Schlenk flask. The mixture was degassed by four freeze-pump-thaw cycles. This reaction mixture was heated in an oil bath at 70ºC for 4 h. Once the targeted polymerization degree was reached, the polymer was precipitated by addition of the solution to ether, and dried under vacuum up to constant weight. The molecular weight was determined by $^1$H NMR in DMSO-d6 ($M_n = 3 \times I_{2.44}/I_{0.8} + 364$), where $I_{0.8}$ and $I_{2.44}$ are the intensities of the proton resonances at 0.8 ppm ($\underline{CH}_3$-$C_{11}H_{22}$, t) and 2.44 ppm ($\underline{CH}$-COOH, m), respectively. Dispersity was measured by size exclusion chromatography (SEC) with a 25 mM solution of LiBr in DMF and found to be 1.10.

*ii. Synthesis of PAA-b-PNIPAM diblock.* Typically, 1 g of trithiocarbonate-capped PAA (PAA-CTA) ($1.75 \times 10^{-4}$ mol for $M_n$ (NMR)= 5.7 kDa and $M_w/M_n$ =1.10), 0.4g of NIPAM ($3.53 \ 10^{-3}$

mol), 10mg of V70 ($3.24\ 10^{-5}$ mol) and 5 mL of DMF were mixed together. The reactive mixture was degassed by four freeze-pump-thaw cycles and the reaction solution was kept stirring at room temperature. The copolymer was precipitated into ether and dried in vacuum up to constant weight. The composition of the second block was determined by $^{1}$H NMR in DMSO-d6 by comparing the peak at 4.01 ppm (N-<u>CH</u><) for the PNIPAM block to the peak at 2.44 ppm (<u>CH</u>-COOH) for PAA block. Dispersity was determined by SEC with a 25 mM solution of LiBr in DMF eluent and calibrated with polystyrene standards. Composition and dispersity of the three copolymers are summarized in Table 1.

**Table 1.** Characteristics of PAA-b-PNIPAM block copolymers (F10, F11 and F22)  used in this study.

| PAA-b-PNIPAM **Block copolymers** | Average degree of polymerization $\overline{\text{DP}}$ | | Mw/Mn* | $\dfrac{\overline{\text{DP}_{\text{PNIPAM}}}}{\overline{\text{DP}_{\text{PAA}}}}$ |
|:---:|:---:|:---:|:---:|:---:|
| | **PAA** | **PNIPAM** | | |
| F10 | 80 | 19 | 1.1 | 0.25 |
| F11 | 80 | 97 | 1.1 | 1.2 |
| F22 | 186 | 136 | 1.3 | 0.75 |

*Dispersities of diblock copolymers as determined by SEC

*2.3. Assembly of polyelectrolyte multilayers (PEMs).* Polyelectrolyte solutions at a concentration of 1 mg mL$^{-1}$ were prepared in 100 mM acetate (pH=5.70 ± 0.05). The build-up of multilayers was performed by alternately dipping a flat substrate in freshly prepared PAH and PAA or PAA-b-PNIPAM solutions for 5 min each. An intermediate rinsing step was performed in two different baths (2 min each) with the buffer solution used for the LbL assembly. This process was repeated until the desired number of bilayers (n) was obtained. The resultant films are thus denoted as "(PAH/PAA)$_n$" or "(PAH/PAA-b-PNIPAM)$_n$".

For incubation tests performed after the build-up of PEMs, samples were immersed in acetate solutions (100 mM) adjusted to pH 3.9 ; 5.7 or 7.3 (by adding acetic acid or sodium hydroxide ) at 20 or 50 °C during 2h.

### 2.4. Characterization of PEMs.

*Ellipsometry.* The substrates used were pieces (∼ 1 cm$^2$) of silicon wafers (ACM, France), cleaned prior to use in a piranha solution (H$_2$SO$_4$ (98%) / H$_2$O$_2$ (30%) 1/1 v/v. *Caution! piranha solutions react violently with organic materials and should not be stored in closed containers*). The substrates were then extensively rinsed with MilliQ water and dried under a nitrogen gas flow. The build-up of (PAH/PAA)$_n$ or (PAH/PAA-b-PNIPAM)$_n$ multilayers was carried out using the procedure described above. The film was additionally rinsed with ultrapure water and dried under nitrogen gas flow. The thickness of dried multilayers was measured using an Uvisel spectroscopic ellipsometer (Horiba-Jobin-Yvon, France) at the fixed angle of incidence of 70° and at wavelengths ranging from 400 to 850 nm. The obtained ellipsometric data were fitted by the software provided by the supplier, using the following model: Si-substrate/SiO$_2$ layer/adsorbed multilayers/air. In this model, the multilayers are assumed to be an unknown, homogeneous and isotropic layer, with a total thickness *d* and a mean refractive index *n*. The optical constants of Si, SiO$_2$ and air were provided by the manufacturer. The transparent Cauchy function was used to model the refractive index of multilayers according to:

$$n\,(\lambda) = A + 10^4\,B\,\lambda^{-2} + 10^9\,C\,\lambda^{-4} \qquad (1)$$

with A, B and C, three fitting parameters.

The evaluated ellipsometric thickness was an average of four measurements, carried out at different spots on the surface of each sample.

*Quartz crystal microbalance with dissipation monitoring (QCM-D).* The build-up of (PAH/PAA)$_n$ or (PAH/PAA-b-PNIPAM)$_n$ multilayers was investigated *in situ* by means of QCM-D. Measurements were carried out using a Q-Sense E4 System (Gothenborg, Sweden) at a temperature of $20.0 \pm 0.1$°C. The sensor used was a thin AT-cut quartz crystal coated with a thin SiO$_2$ film (thickness ~ 50 nm) provided by Q-Sense (QSX 303). It was cleaned with 2% (v/v) solution of Hellmanex (Fluka, Germany), MilliQ water and ethanol, and dried with nitrogen gas flow. The sensors were then placed under UV/O$_3$ treatment for 20 min and again rinsed with ethanol and dried with nitrogen. The oscillations of the crystal at the resonant frequency (5 MHz) or at one of its overtones (15, 25, 35, 45, 55 MHz) were obtained when applying ac voltage. The variations of the resonance frequency ($\Delta f$) and of dissipation ($\Delta D$) were monitored upon adsorption of the polyelectrolytes. Solutions were introduced into the measurement cell using a peristaltic pump (Ismatec IPC-N 4) at a flow rate of 50 $\mu$L min$^{-1}$. Prior to the multilayer build-up, acetate buffer solution was injected to establish the baseline. The growth of (PAH/PAA)$_n$ or (PAH/PAA-b-PNIPAM)$_n$ multilayers was performed as follows: first, PAH solution was introduced into the measurement cell during 15 min. Subsequently, rinsing was performed for 15 min using acetate buffer solution. PAA or PAA-b-PNIPAM was then injected following the same procedure used for PAH. For protein adsorption tests, solution of ovalbumin, prepared in acetate buffer at the desired concentration (0.2 ; 1.0 or 25.0 mg mL$^{-1}$), was injected during 30 min after the build-up of (PAH/PAA)$_4$ or (PAH/PAA-b-PNIPAM)$_4$ multilayers followed by rinsing with buffer. Protein adsorption was carried out either at 20 or 50 °C. For this purpose, temperature was increased from 20 to 50 °C at a constant rate of 0.5 °C min$^{-1}$, then maintained at 50 °C for 1 h before the injection of protein solution.

*Polarization-modulation infrared reflection-absorption spectroscopy (PM-IRRAS)*. PM-IRRAS analyses were performed on gold-coated substrates (~1 cm$^2$) prepared by metallization of silicon wafer (ACM, France) with 10 nm titanium layer, to enhance the adhesion of gold on the silicon surface, and 100 nm of gold layer on top. The samples were cleaned before use in piranha during 10 min, then rinsed in water and dried under nitrogen gas flow. PM-IRRAS spectra were collected in the wavenumber range of 3400-1000 cm$^{-1}$ using a commercial NICOLET Nexus spectrometer. Under optimal conditions (incident angle of 80°) the external beam was focused on the sample with a mirror. A ZnSe grid polarizer and a ZnSe photoelastic modulator to modulate the incident beam between p and s polarizations (HINDS Instruments, PM90, modulation frequency = 37 kHz) were placed prior to the sample. The light reflected on the sample was then focused in a N$_2$ cooled MCT (HgCdTe) wide band detector. Using the modulation of polarization enables rapid analyses of samples to be performed without purging the atmosphere or requiring a reference spectrum. Presented spectra were obtained from the sum of 128 scans recorded with a resolution of 8 cm$^{-1}$. The measured data were corrected using the software (OMNIC) provided by the supplier.

## 3. Results and discussion

### 3.1. Build-up of (PAH/PAA-b-PNIPAM)$_n$ multilayers.

The state of PAA-b-PNIPAM in solution prior to the LbL assembly has to be taken into account. According to Schilli et al., PAA-b-PNIPAM may form micelles or other aggregates in aqueous solution depending on temperature and pH of the medium [23]. Micelles with a PNIPAM core and PAA corona are formed at pH > 4 and T > LCST where the PAA is deprotonated and PNIPAM is collapsed. At T < LCST and pH values lower than ~4, micelles with a protonated PAA core

and PNIPAM corona are formed. The formation of aggregates or a gel-like structure may also occur in the latter pH range by increasing the temperature below the LCST. It appears that the factors influencing the behavior of PNIPAM-PAA block copolymers in solution are : (i) protonation/deprotonation of AA, collapsing/swelling of NIPAM units and (iii) hydrogen bonding between the two blocks. In the conditions used in the present study, the LbL sequential assembly is performed at room temperature, i.e. T < LCST and pH ~5.7. In these conditions of temperature and pH, the micellar state is not the most stable form. The predominant form of PAA-b-PNIPAM is thus unimers rather than BCMs, but the formation of aggregates could not be fully ruled out.

The growth of $(PAH/PAA)_n$ and $(PAH/PAA-b-PNIPAM)_n$ multilayers was first monitored by ellipsometry measurements based on the estimation of the film thickness in the dried state. As already reported in the literature, due to the fact that PAH and PAA contain ionizable amine and carboxylic acid functions, respectively, the growth of $(PAH/PAA)_n$ multilayers is strongly pH-dependent [5, 25]. In this work, $(PAH/PAA)_n$ and $(PAH/PAA-b-PNIPAM)_n$ multilayers were built in acetate buffer at a pH of 5.7. At this pH, the thickness of all films is increasing progressively as a function of the number of bilayers, n (Figure 1A). The thickness of $(PAH/PAA-b-PNIPAM)_4$ films is almost the same for all block copolymers (F10, F11 and F22), but was noticeably higher than the one obtained for $(PAH/PAA)_4$.
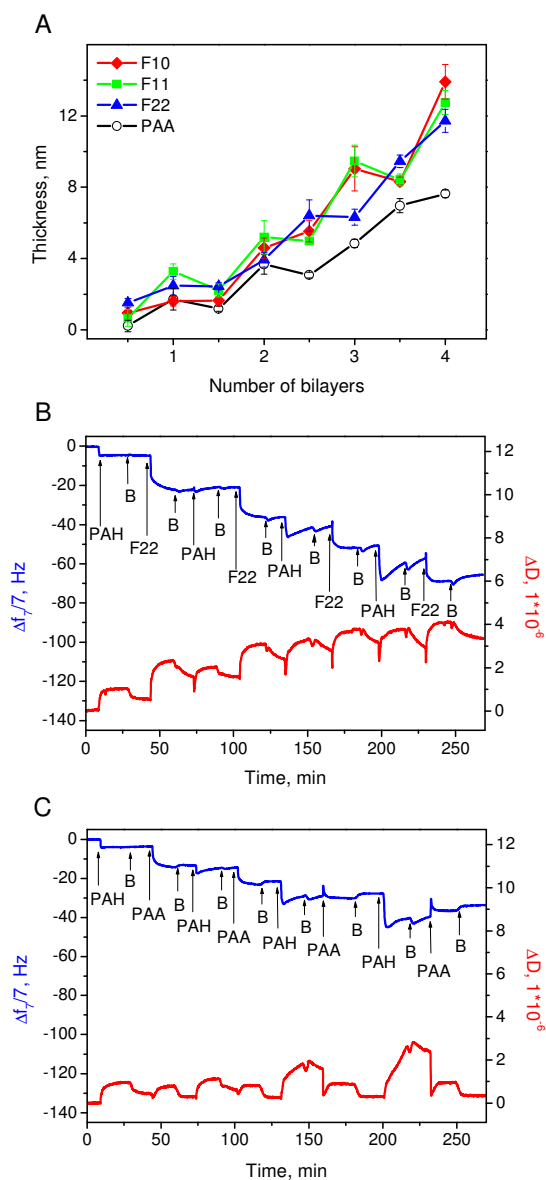
**Figure 1.** (A) Ellipsometry measurements showing the evolution of the thickness of (PAH/PAA)$_n$ and the different (PAH/PAA-b-PNIPAM)$_n$ multilayers, using F10, F11 or F22 as block copolymers. All multilayers were built-up in acetate buffer at pH=5.7. (B) and (C) Representative QCM-D measurements showing frequency changes in the 7$^{th}$ overtone and the corresponding dissipation during the build-up of (PAH/F22)$_n$ and (PAH/PAA)$_n$ multilayers in acetate buffer (pH=5.7).

The growth of block copolymer-based multilayers was also monitored *in situ* in the hydrated state by means of QCM-D. A shift of the resonant frequency is observed for each added layer, corresponding to the adsorption of PAH and F22 copolymer (Figure 1B). These results clearly confirm the growth of (PAH/PAA-b-PNIPAM)$_n$ multilayers in a similar way than (PAH/PAA)$_n$ (Figure 1C), proving the possibility to incorporate the block copolymer in LbL assembly as a polyanion in the chosen experimental conditions (data not shown for F11 and F10). Both the frequency and dissipation shifts recorded after 4 bilayers are significantly higher for block copolymer-containing LbL film compared to PAA-containing LbL film. This result is in perfect agreement with ellipsometry observations showing a higher thickness of the (PAH/F22)$_n$ film, compared to (PAH/PAA)$_n$ film.

PM-IRRAS spectra (Figure 2) were recorded on (PAH/PAA)$_4$ and (PAH/PAA-b-PNIPAM)$_4$ films in the dried state and reveal the presence of characteristic bands of the polymers involved in the LbL assemblies. The C-H stretching modes of methylene groups, $\nu_{as}(CH_2)$ at 2932 cm$^{-1}$ is observed. The asymmetric stretching mode of CH$_3$ moieties, $\nu_{as}(CH_3)$, is also visible at 2975 cm$^{-1}$ and the broadening near 2875 cm$^{-1}$ can be attributed to the corresponding symmetric mode, $\nu_s(CH_3)$. These vibrational features are mainly attributed to the alkyl chains of the adsorbed polymers. The low frequency region is dominated by characteristic bands of amide and carboxylic groups. Vibration band associated with the symmetric stretching modes of COO$^-$ moiety at about 1404 cm$^{-1}$ is clearly visible, in addition to a band at 1467 cm$^{-1}$ which may be attributed to $\delta(CH_2)$. The band at 1713 cm$^{-1}$ is attributed to $\nu(C=O)$ originating from carboxylic acid moieties in PAA as well as in PAA-b-PNIPAM. Bands at 1649 and 1559 cm$^{-1}$ corresponding to amide I and amide II, respectively, come from the PNIPAM units. The exploitation of these specific bands is complex owing to the overlapping of antisymmetric modes

of the COO$^-$ moiety (around 1546 cm$^{-1}$) and vibrational features of –NH$_2$ groups from PAH. However, based on the relative variations of intensities of bands at 1559 and 1649 cm$^{-1}$, clear differences between block copolymer- and PAA-containing PEMs are appearing. Indeed, the presence of PNIPAM units leads to an increase of the intensity of amide I band compared to amide II band (Figure 2, right). This trend is even more pronounced for F11 copolymer that possesses a DP$^{PNIPAM}$/DP$^{PAA}$ ratio higher than 1 (Table 1), compared to F10 and F22.
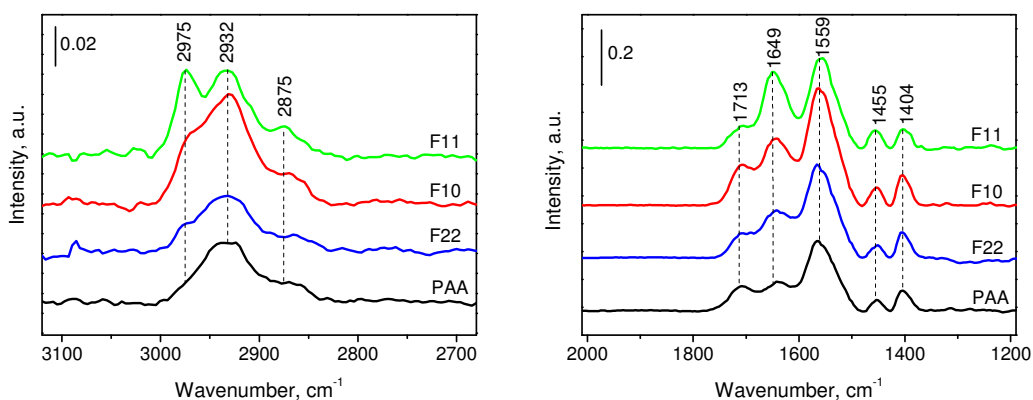


**Figure 2.** PM-IRRAS spectra recorded after the build-up of (PAH/PAA)$_4$ and (PAH/PAA-b-PNIPAM)$_4$ multilayers in acetate buffer (pH=5.7) at high (left) and low (right) frequency regions.

To monitor the build-up of the LbL films, PM-IRRAS spectra were also recorded after the deposition of each layer, showing noticeable increase of characteristic band intensities as a function of the number of bilayers (Figure S1, supporting information). The pK$_a$ of PAA in solution is found to be around 5.7 – 6.5 [4, 26, 27]. When incorporated in PEMs, pK$_a$ shifts toward more acidic values to reach, for instance, ~ 4.5 in a PAA monolayer [28] and can decrease further as a function of the number of layers [29]. This trend is mainly due to molecular interactions of charges with opposite sign charges within PEM that are stabilizing the deprotonated form. As IR techniques are sensitive to the dissociation degree of weak polyacids, we have roughly estimated

14

the degree of protonation of –COOH moieties in adsorbed PAA using the intensity of $\nu$(C=O) and $\nu_s$(COO$^-$) bands located at 1713 and 1404 cm$^{-1}$, respectively (see supporting information, Table S1, supporting information). The degree of ionization of PAA could not be determined with accuracy using PM-IRRAS data, as the intensity of the band due to $\nu_{as}$(COO$^-$) is overlapping with amide I band, as described above. But, though this approach is not quantitative, it allows comparing samples. At pH = 5.7, PAA and PAA-b-PNIPAM-containing PEM present a fraction of ionized PAA ranging from about 0.30 to about 0.38 (Table S1).

So, as evidenced both in the dried and hydrated states, the presence of PNIPAM segments does not disturb the process of self-assembly and allows the growth of (PAH/PAA-b-PNIPAM)$_4$ films. This indicates that, despite the presence of PNIPAM segments, enough -COO$^-$ groups from PAA remain accessible for interaction with the subsequent layer of polycation.

### 3.2. Effect of the temperature

Prior to protein adsorption study, the impact of temperature on the PEMs after their build-up (4 bilayers) was studied using ellipsometry measurements. For this purpose, PEM were incubated in acetate buffer at pH~5.7 for 2h. Results show that increasing the temperature from 20 to 50°C does not significantly influence the thickness of (PAH/PAA)$_4$ film and induces only a slight decrease of the  (PAH/F22)$_4$ multilayer film (Figure 3).

**Soft Matter Accepted Manuscript**
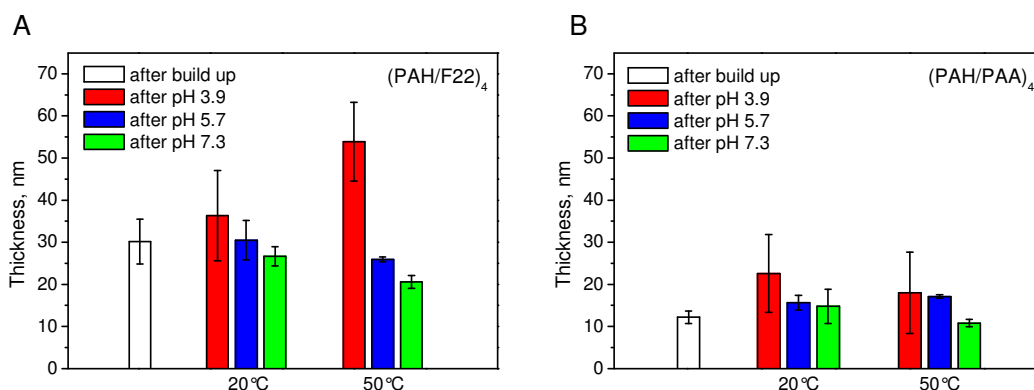
**Figure 3.** Ellipsometric thickness of (PAH/F22)$_4$ (A) and (PAH/PAA)$_4$ (B) LbL films performed at pH=5.7 prior to and after further incubation in acetate solutions adjusted at pH = 3.9; 5.7 and 7.3 at 20 and 50 °C.

The adsorption behavior of ovalbumin at pH=5.7 was then investigated at two different temperatures (below and above PNIPAM LCST) on (PAH/PAA)$_4$ and on the three different (PAH/PAA-b-PNIPAM)$_4$ films. Protein adsorption, from solutions of different concentrations, was monitored using QCM-D measurements at 20 and 50°C. It is noteworthy that, at the higher studied temperature, ovalbumin is not denatured [30]. Figure 4 shows the evolution of the frequency shift on (PAH/PAA)$_4$ and (PAH/F22)$_4$ films. At 20°C the adsorption is weak on (PAH/PAA)$_4$ (frequency shift does not exceed the value of ~ -10Hz with low dissipation), while no frequency shift is detected on (PAH/PAA-b-PNIPAM)$_4$. By contrast, when the adsorption of proteins is performed at 50$^0$C, noticeable frequency shifts are observed on both types of films. Interestingly, the recorded Δf is higher when the block copolymer is present in the LbL film. From QCM-D monitoring, it also appears that the adsorption kinetics is significantly slower on (PAH/PAA)$_4$ compared to (PAH/F22)$_4$, keeping in mind that a presumable effect of flow on mass transport limitations can be considered to be similar for both systems. Furthermore, the

rinsing leads to a frequency shift in the opposite way only on (PAH/PAA)$_4$ film, suggesting a partial desorption of proteins.
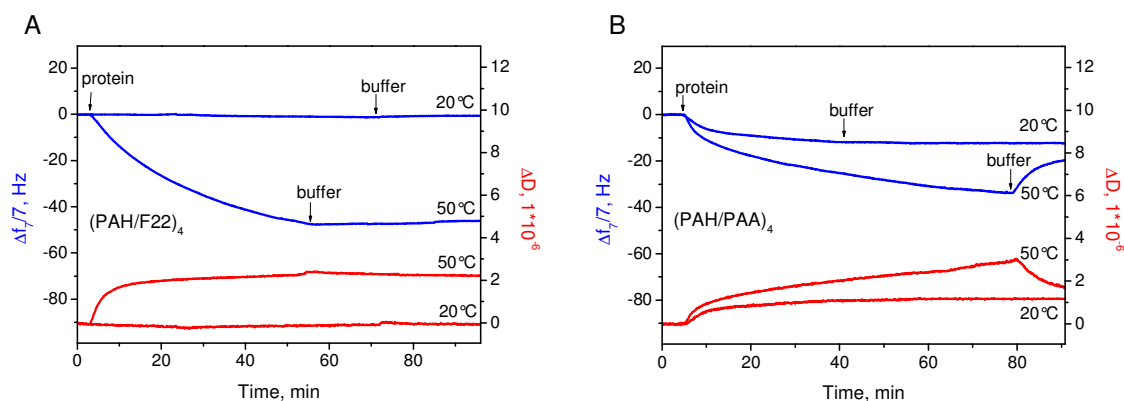


**Figure 4.** Representative QCM-D measurements showing frequency changes in the 7$^{th}$ overtone and the corresponding dissipation vs time during the adsorption of ovalbumin (0.2 mg ml$^{-1}$) on (PAH-F22)$_4$ (A) and (PAH-PAA)$_4$ (B). Protein adsorption was performed in acetate buffer either at 20 or 50$^0$C, as indicated.

QCM-D data obtained using different concentrations of proteins and different block copolymers are summarized in Table 2. The frequency shifts reported were measured between two baselines established in buffer, prior to protein adsorption and after adsorption and subsequent rinsing. Though (PAH/PAA)$_4$ film limits the adsorption of protein at 20$^0$C, block copolymer-containing films are more efficient at both temperatures. On the one hand, these films limit the adsorption of OVA at 20 $^0$C, or completely prevent it in the case of F22 at 0.2 mg mL$^{-1}$ (at least at the detection limit of QCM-D ~ 1-2 Hz) , and on the other hand, they strongly favor the protein adsorption when increasing the temperature to 50$^0$C (T above the LCST of PNIPAM).

**Table 2.** QCM-D frequency shifts (absolute values) for the $7^{th}$ overtone (in Hz), recorded after the interaction of ovalbumin (OVA) at concentration of 0.2, 1.0, and 25.0 mg mL$^{-1}$ with (PAH/PAA)$_4$, (PAH/F10)$_4$, (PAH/F11)$_4$ and (PAH/F22)$_4$ multilayers in acetate buffer (pH ~5.7) during 40 to 80 min at 20 and 50$^0$C.

| LbL films | $C_{OVA}$=0.2 mg mL$^{-1}$ | | $C_{OVA}$=1 mg mL$^{-1}$ | | $C_{OVA}$=25 mg mL$^{-1}$ | |
|---|---|---|---|---|---|---|
| | 50$^°$C | 20$^°$C | 50$^°$C | 20$^°$C | 50$^°$C | 20$^°$C |
| PAA | 19.7 | 12.5 | 42.1 | 29.7 | 93.6 | 54.1 |
| F10 | 29.3 | 4.3 | 81.5 | 15.9 | 246.4 | 48.1 |
| F11 | 43.9 | 5.6 | 71.6 | 14.8 | 211.3 | 3.3 |
| F22 | 45.9 | bdl | 90.4 | 9.9 | 122.1 | 15.3 |

bdl – below detection limit

A more quantitative evaluation of the thermoresponse behavior of LbL films in terms of their interaction with proteins can be obtained by comparing data obtained at 20 and 50$^0$C. For this purpose, a heuristic parameter is defined as follows:

$$R = \frac{\Delta f^{50} - \Delta f^{20}}{\Delta f^{50}} \times 100 \tag{2}$$

where $\Delta f^{50}$ and $\Delta f^{20}$ are the frequency shifts recorded as a result of the protein adsorption on the polyelectrolyte multilayers at 20 and 50 °C, respectively.

This parameter provides direct information regarding the performance of the LbL films to tune protein adsorption according to the temperature of the medium. The evolution of R in terms of the concentration of protein solution is given in Figure 5. The R values are significantly lower for (PAH/PAA)$_4$ compared to (PAH/PAA-b-PNIPAM)$_4$ films regardless of the protein

18

concentration and of the block copolymer used. Indeed, the R values range from 80 to 98% for

PAA-b-PNIPAM films and vary from about 29 to 42% for PAA-based films (Figure 5). This

clearly indicates the ability of PNIPAM containing coatings to efficiently control protein

adsorption based on temperature
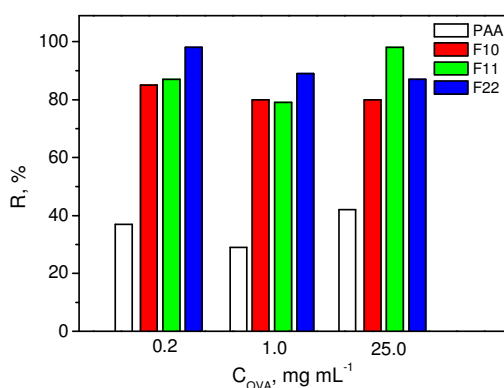


**Figure 5.** Performances of PEM, as indicated, through the evolution of R ratio (%) obtained after adsorption of ovalbumin (at concentrations $C_{OVA}$ = 0.2; 1 and 25 mg.mL$^{-1}$) on (PAH-F10)$_4$, (PAH-F11)$_4$, (PAH-F22)$_4$ or (PAH-PAA)$_4$ films in acetate buffer (pH ~5.7) during 40 to 80 min at 20$^0$C and 50$^0$C.

The mechanism of interaction of proteins with polyelectrolyte multilayers has been described in

the literature [31-34]. Factors influencing this process, such as thickness and surface charge of the

multilayers, ionic strength and pH of the solution, have been investigated. According to Salloum

and Schlenoff, there is a variety of possible mechanisms regarding the protein interaction with

PEMs, including adsorption on the top of the film or absorption within the multilayers [35]. These

conclusions were drawn using strong polyelectrolytes and by investigating the effect of the PEM

thickness (number of bilayers) on the adsorbed amount of proteins. In the present study, the

frequency shifts obtained by QCM-D on 4 bilayers PEMs at 50°C (when protein adsorption is

promoted) tend to indicate that proteins are only adsorbed on top of the films and that the formation of protein multilayers and their interdiffusion within PEMs are quite unlikely.

On PNIPAM brushes, an increase of the solution temperature leads to a coil-to-globule transition that affects the surface wettability [36] and consequently, the adsorption behavior of proteins. In the present PAH/PAA-b-PNIPAM studied system, PNIPAM units are included in a block copolymer structure and further, incorporated in a multilayered film. Though this can inhibit the chains mobility and the coil-to-globule transition processes, our results clearly prove the ability of the (PAH/PAA-b-PNIPAM)$_4$ films to switch from favorable (at 50 °C) to unfavorable (at 20 °C) configuration with regard to ovalbumine adsorption. On (PAH/PAA)$_4$, this trend is also observed but remains less pronounced compared to (PAH/PAA-b-PNIPAM)$_4$, demonstrating the strong impact of PNIPAM moieties in the observed thermo-control of protein adsoprtion.

### 3.3. Effect of pH

As previously mentioned, there is an abundant literature on the high sensitivity of (PAH/PAA)$_n$ multilayers to pH changes, owing to their acid-base properties (weak polyelectrolytes). However, from the available data, it is important to discriminate between (i) the effect of pH used for the build-up (pH of polyelectrolyte solutions) of the LbL film and (ii) pH changes of the medium used after the film was completely built (post-treatment). The first effect is widely reported in the literature [5, 25]. In the present study, we are focusing on the second effect. Protein adsorption was performed at different pH values: the pH used for LbL film build-up (5.7), a more acidic pH (~3.9) and a more basic pH (~8.1), while keeping the temperature constant, either at 20 or 50°C. Prior to protein adsorption tests, the evolution of the multilayered film structure upon incubation in simple acetate solutions adjusted at the different pH values was carefully studied. Ellipsometry

measurements show that an increase of the pH leads to a slight decrease of the film thickness for both PAA- and PAA-b-PNIPAM containing films, independently of the temperature (Figure 3). At acidic pH, an increase of the thickness of both films is observed, in particular, for (PAH/F22)$_4$ system at 50 °C where the film thickness increases from about 30 nm (at pH= 5.7) to about 55 nm (at pH 3.9). This result indicates that the structure of (PAH/F22)$_4$ is not only sensitive to pH and T stimuli in a separated way but is also subject to a synergistic effect between both parameters. The film structure modifications can include a combination of (i) loops and tails conformation due to the protonation of PAA moieties and, (ii) coil-to-globule transition of PNIPAM groups upon temperature change (see discussion below).

More direct evidences regarding the degree of protonation of carboxyl groups is provided by PM-IRRAS analyses (Figure 6). The intensity of the band at about 1711 cm$^{-1}$ due to $\nu$(C=O) increases markedly at pH = 3.9, suggesting the protonation of carboxylate groups of PAA incorporated in the PEM. As a consequence, the fraction ionized PAA decreases markedly as shown in Table S1 (supporting information). The noticeable increase of the (PAH/F22)$_4$ film thickness at pH 3.9 particularly at 50 °C is consistent with this assumption. The formation of loop-and-tail conformations can provide more freedom degree to PNIPAM units within the PEM, which should facilitate their response to temperature stimulus.

According to Shiratori and Rubner, [5] in (PAH/PAA)$_n$ multilayers, when PAA is deprotonated it strongly interacts with PAH, thus adapting a "flat" configuration called train-like segments. By contrast, the protonation of PAA decreases the "points" of interaction between PAA and PAH and leads to the formation of the so-called loops and tails. Upon drying, PEMs containing loops and tails exhibit higher surface roughness. [5] In the present study, in addition to the increase of the film thickness, upon incubation in the acidic medium, standard deviations are significantly

higher compared to other conditions (Figure 3). This may be due to an increase of the surface roughness, thus supporting the fact that both (PAH/PAA)$_4$ and (PAH/PAA-b-PNIPAM)$_4$ multilayers include of a significant population of loops and tails.
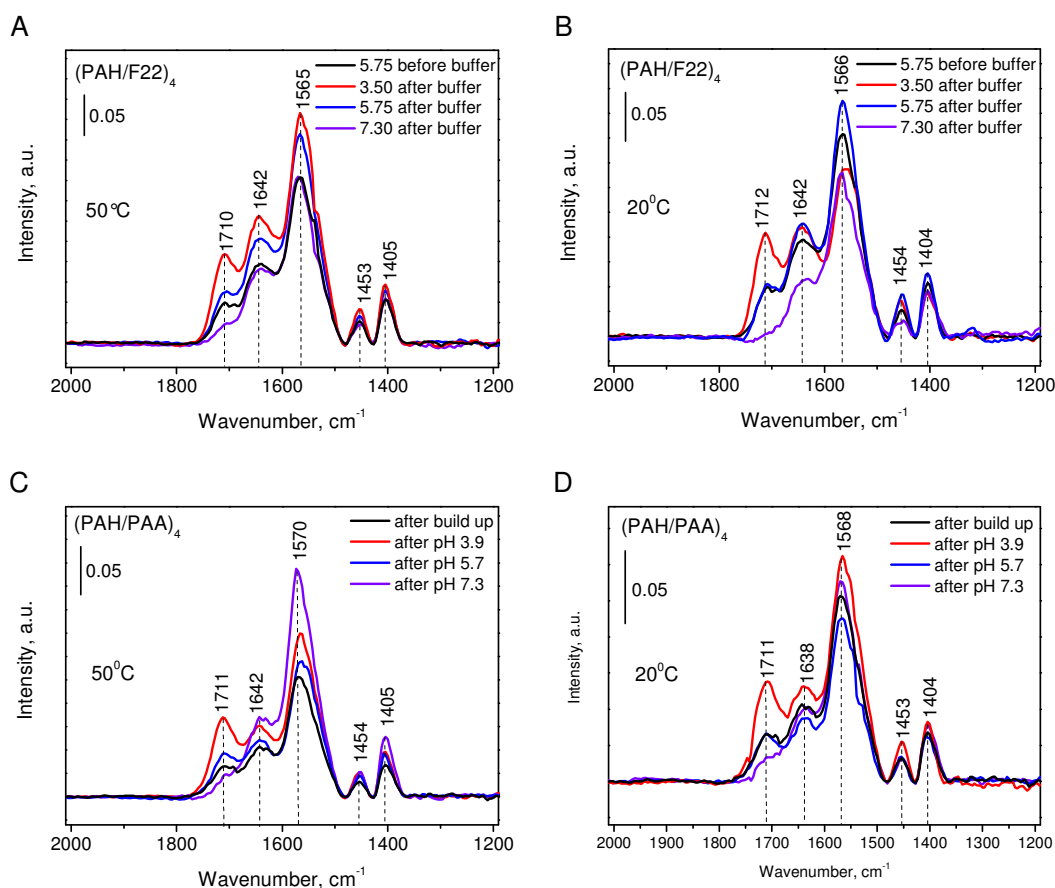


**Figure 6.** PM-IRRAS spectra recorded on (PAH/F22)$_4$ (A, B) and (PAH/PAA)$_4$ (C, D) films built-up at pH=5.7 before and after immersion in a 100 mM acetate solutions adjusted to pH 3.9 and 7.3 at 20 and 50$^0$C.

The adsorption of ovalbumin in the different pH and T conditions was monitored by means of QCM-D measurements. Typical frequency and dissipation signals recorded on (PAH/PAA)$_4$ and (PAH/PAA-b-PNIPAM)$_4$ films are given in supporting information (Figure S2, supporting information). Frequency shifts obtained after protein injection and subsequent rinsing are

22

summarized in Table 3. In some cases, no frequency shift is observed after the injection of

protein solution, suggesting that the amount of adsorbed proteins is below the detection limit

(bdl) of the technique. Again, the parameter R (equation 1) is used to evaluate the ability of PEM

for protein adsorption/repellency at 50 and 20 °C at each pH condition and using two protein

concentrations (Figure 7).

**Table 3.** QCM-D frequency shifts (absolute values) for the 7th overtone, recorded after the interactions of ovalbumin at concentration of 0.2 and 25.0 mg mL^{-1} with (PAH/PAA)$_4$, (PAH/F11)$_4$ and (PAH/F22)$_4$ multilayers at 20 and 50[0]C in acetate solutions adjusted at pH 3.9 (acidic) and 8.1 (basic) during 40 to 80 min.

| LbL films | $C_{OVA}=0.2$ mg mL^{-1} | | | | $C_{OVA}=25.0$ mg mL^{-1} | | | |
|---|---|---|---|---|---|---|---|---|
| | acidic | | basic | | acidic | | basic | |
| | 50°C | 20°C | 50°C | 20°C | 50°C | 20°C | 50°C | 20°C |
| PAA | 185.6 | 8.5 | bdl | bdl | 853.0 | 117.2 | 10.6 | 12.0 |
| F11 | 157.2 | 7.3 | bdl | bdl | 729.5 | 51.4 | 49.4 | 7.7 |
| F22 | 183.6 | bdl | bdl | bdl | 461.2 | 10.4 | 17.7 | bdl |

At pH = 8.1, the interactions of OVA with PEMs are weak (Table 3), independently of the

temperature. At high concentrated protein solution ($C_{OVA}$ = 25 mg mL^{-1}), the frequency shifts are

significantly lower compared to the values recorded at pH= 5.7 (Table 2), while at low protein

concentration ($C_{OVA}$ = 0.2 mg mL^{-1}), the values are below the detection limit. This could be

explained by the electrostatic repulsion between negatively charged surface groups (carboxylic

groups of PAA being mostly deprotonated) and negatively charged residues of proteins. This

observation is in agreement with Salloum and Schlenoff findings that suggest electrostatic

repulsion between bovine serum albumin and PAH/PAA multilayers at pH=7.4 [35]. In contrast,

Ladam et al. observed that proteins might interact with PEMs whatever the exposed charge of

both. Though, when PEMs exhibit charges of the same sign as proteins, the adsorbed amount is extremely low compared to the case where the charges of proteins and PEMs are opposite [37].

At pH 3.9, the frequency shift is quite high (Table 3), as well as dissipation (Figure S2, supporting information), particularly when using high concentration of OVA (25 mg mL$^{-1}$). This could result from the penetration of proteins within the film, or the adsorption of a large amount of proteins on the top of PEMs, probably in the form of protein multilayers. The latter phenomenon can indeed occur when electrostatic repulsive forces are minimal, for instance, when adsorption is performed at pH close to the isoelectric point (iep) of proteins [38]. In the present study, regarding the iep of OVA, it is noteworthy that experimental values ranging from 4.7 to 4.9 have been reported [39-41] and that the theoretical iep computed on the basis of the amino acid composition of OVA, using ProtParamtool tool is 5.1 [42]. Accordingly, in all cases, the iep of OVA falls between pH= 3.9 and pH= 5.7. Though, at pH=5.7, the adsorption behavior of OVA is completely different from the one observed at pH = 3.9 (Figure S3) and no accumulation of high amount of proteins is observed.

These results reveal that electrostatic interactions are not solely responsible for the significant increase of adsorbed amount of proteins in acidic conditions at 50°C. The most likely explanation is that, at pH=3.9, PEM film offers the possibility to adsorb a very high amount of proteins owing to its tendency to reorganize into thicker and swollen film, as described above [5, 43].

24
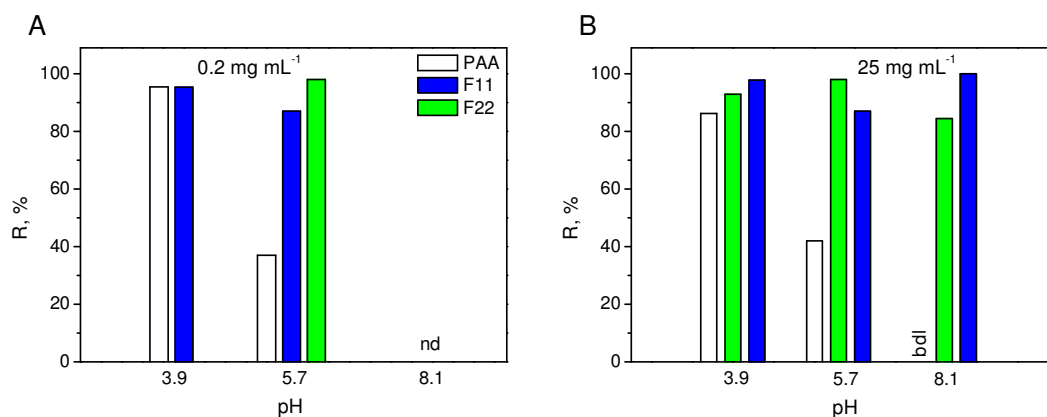
**Figure 7.** Performances of LbL films as indicated by the evolution of R ratio (%) (see equation 1) obtained after adsorption of ovalbumin (at concentrations of 0.2 and 25 mg.mL$^{-1}$) on (PAH-F11)$_4$, (PAH-F22)$_4$ or (PAH-PAA)$_4$ in acetate solutions adjusted at pH = 3.9; 5.7 and 8.1, at 20 and 50°C. ("bdl" = below detection limit; "nd" = not defined).

Actually, when the protein adsorbed amount is as high as the one observed here at acidic pH (3.9), it is hard to conclude whether proteins are accumulating on top of the film (multilayers) or penetrating within the film or both. This issue was approached in previous investigations by tuning the surface charge of the outermost part of the PEM. Some authors have shown a linear increase of the amount of BSA with the number of bilayers when the PEM is terminated with the opposite charge of BSA (attractive). By contrast, the amount of BSA remains low and independent of the multilayer thickness when the PEM surface exhibits the same charge as BSA [35]. These findings are also in agreement with previous observations made on IgG by Caruso et al. and on lysozyme by Rubner et al. [44, 45]. Therefore, to rationalize the mechanism of penetration of proteins into PEM, the surface charges of entities in interaction (proteins and outermost layer of PEM) has to be taken into account in addition to the film structure.
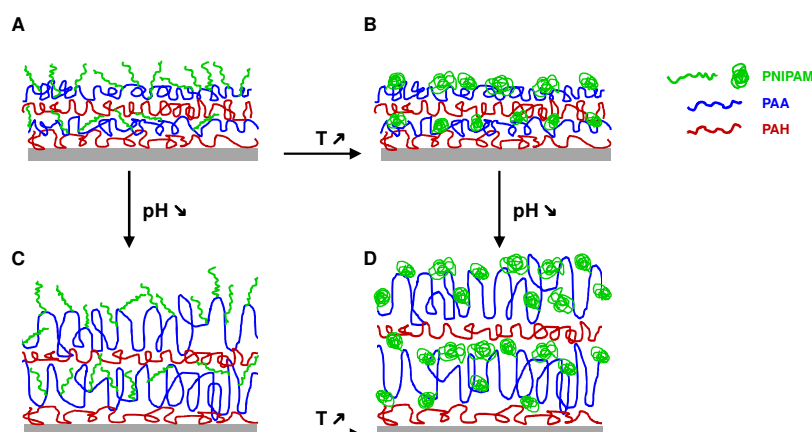
**Figure 8.** Schematic representation illustrating the evolution of PAH/PAA-b-PNIPAM multilayers (2 bilayers) upon changes in temperature (20 and 50°C) and pH (~3.9 and ~5.7).

These conclusions were validated for simple polyelectrolyte pairs. The situation with $(PAH/PAA)_n$ and $(PAH/PAA\text{-}b\text{-}PNIPAM)_n$ multilayers is, however, more complex. Our results evidence that pH strongly influences film thickness and probably its permeability, in agreement with previous findings [4, 25, 46, 47]. For instance, at low pH values, PAH/PAA-b-PNIPAM multilayers are expected to exhibit a swollen and highly hydrated state, as observed for $(PAH/PAA)_n$ [45]. Accordingly, in addition to concerns related to surface charges (described above), the evolution of the film structure upon interaction with proteins has to be taken into consideration. Based on ellipsometry measurements (Figure 3) and PM-IRRAS analyses (Figure 6), the impact of pH and temperature on the structure of PAH/PAA-b-PNIPAM multilayered film is schematically depicted in Figure 8. This film structure evolution may lead to two antagonist phenomena in regards to protein adsorption behavior. (i) At temperature below PNIPAM LCST, the resulting state of the film, especially its outermost part, is not favorable to protein adsorption as it behaves like a gel structure, containing extensive water in a similar state to bulk water, due to the presence of PNIPAM units (Figure 8A and C). Accordingly, no free

energy can be gained by protein adsorption on PEM, as reported for other molecules which reduce non specific adsorption [48]. (ii) The loop-rich conformation, induced by acidic pH (Figure 8C and D) allows the multilayers to act as a "sponge" to load proteins, thus increasing its capacity to "host" proteins.

The response of PEMs to temperature changes, as indicated through the ratio R (Figure 7), shows relevant performance of block copolymer-containing films, depending on the pH. The most significant effects are observed at pH=5.7 (similar pH than the one used to build-up the film) and at pH=8.1 for the highly concentrated protein solution (Figure 7). By contrast, at pH=3.9, block copolymers provide only a slight effect compared to PAA.

### 4. Conclusion

The formation of a new kind of pH- and thermo-sensitive surface based on LbL sequential assembly of PAH and PAA-b-PNIPAM block copolymer was investigated. PEM, block copolymers presenting different PAA and PNIPAM block lengths were used. A special attention was paid to the investigation of protein adsorption behavior on these various LbL films in terms of the temperature and/or pH changes in the medium. This study highlights the remarkable ability of tuning protein adsorption on PAA-b-PNIPAM multilayered films by adjusting the environment conditions. In particular, at pH=5.7, block copolymer-based films were shown to present enhanced performance compared to PAA/PAH films, allowing adsorption of a large amount of ovalbumin at 50°C and being strongly protein-repellent at 20°C. As a whole, the results of this study provide relevant information regarding a possible synergetic effect of temperature and pH on the PEM/protein interactions.

Furthermore, these PNIPAM block copolymer-based LbL coatings are easy to build on substrates of various nature and geometry (including membranes and micro- or nanoparticles),

and they present highly tunable features. This makes them ideal candidates to be employed for applications requiring the control of protein adsorption, such as protein separation or cell culture.

**Acknowledgment**

28

## References

1.  Philippe Lavalle, Jean-Claude Voegel, Dominique Vautier, Bernard Senger, Pierre Schaaf and V. Ball, *Advanced materials*, 2011, **23**, 1191–1221.
2.  T. Boudou, T. Crouzier, K. Ren, G. Blin and C. Picart, *Adv. Mater.*, 2010, **22**, 441-467.
3.  R. Heuberger, G. Sukhorukov, J. Vörös, M. Textor and H. Möhwald, *Advanced Functional Materials*, 2005, **15**, 357-366.
4.  J. Choi and M. F. Rubner, *Macromolecules*, 2005, **38**, 116-124.
5.  S. S. Shiratori and M. F. Rubner, *Macromolecules*, 2000, **33**, 4213-4219.
6.  K. Itano, J. Choi and M. F. Rubner, *Macromolecules*, 2005, **38**, 3450-3460.
7.  S. E. Burke and C. J. Barrett, *Macromolecules*, 2004, **37**, 5375-5384.
8.  M. Heskins and J. E. Guillet, *Journal of Macromolecular Science: Part A - Chemistry*, 1968, **2**, 1441-1455.
9.  F. D. Jochum and P. Theato, *Chemical Society reviews*, 2013, **42**, 7468-7483.
10. M. A. Cooperstein and H. E. Canavan, *Langmuir*, 2009, **26**, 7695-7707.
11. S. Burkert, E. Bittrich, M. Kuntzsch, M. Muller, K. J. Eichhorn, C. Bellmann, P. Uhlmann and M. Stamm, *Langmuir*, 2010, **26**, 1786-1795.
12. M. A. Cole, M. Jasieniak, H. Thissen, N. H. Voelcker and H. J. Griesser, *Analytical Chemistry*, 2009, **81**, 6905-6912.
13. S. Pavlukhina and S. Sukhishvili, *Advanced Drug Delivery Reviews*, 2011, **63**, 822-836.
14. K. Matyjaszewski and J. Xia, *Chemical Reviews*, 2001, **101**, 2921-2990.
15. G. B. Webber, E. J. Wanless, S. P. Armes, Y. Tang, Li, Y.  and S. Biggs, *Adv. Mater.*, 2004, **16**, 1794-1798.
16. T. Tang, V. Castelletto, P. Parras, I. W. Hamley, S. M. King, D. Roy, S. Perrier, R. Hoogenboom and U. S. Schubert, *Macromolecular Chemistry and Physics*, 2006, **207**, 1718-1726.
17. S. Cammas, K. Suzuki, C. Sone, Y. Sakurai, K. Kataoka and T. Okano, *Journal of Controlled Release*, 1997, **48**, 157-164.
18. F. Kohori, K. Sakai, T. Aoyagi, M. Yokoyama, Y. Sakurai and T. Okano, *Journal of Controlled Release*, 1998, **55**, 87-98.
19. I. Erel, Z. Zhu, S. Sukhishvili, E. Patyukova, I. Potemkin and E. Kramarenko, *Macromolecular Rapid Communications*, 2010, **31**, 490-495.
20. Z. Zhu and S. A. Sukhishvili, *ACS Nano*, 2009, **3**, 3595-3605.
21. L. Xu, Z. Zhu and S. A. Sukhishvili, *Langmuir*, 2011, **27**, 409-415.
22. I. Erel, Z. Zhu, A. Zhuk and S. A. Sukhishvili, *Journal of colloid and interface science*, 2011, **355**, 61-69.
23. C. M. Schilli, M. Zhang, E. Rizzardo, S. H. Thang, Y. K. Chong, K. Edwards, G. Karlsson and A. H. E. Müller, *Macromolecules*, 2004, **37**, 7861-7866.
24. A. Aqil, S. Vasseur, E. Duguet, C. Passirani, J. P. Benoit, R. Jerome and C. Jerome, *Journal of Materials Chemistry*, 2008, **18**, 3352-3360.
25. P. Bieker and M. Schönhoff, *Macromolecules*, 2010, **43**, 5052-5059.
26. L. Bromberg, *The Journal of Physical Chemistry B*, 1998, **102**, 10736-10744.
27. O. E. Philippova, D. Hourdet, R. Audebert and A. R. Khokhlov, *Macromolecules*, 1997, **30**, 8278-8285.
28. P. Bieker and M. Schönhoff, *Macromolecules*, 2010, **43**, 5052-5059.
29. S. E. Burke and C. J. Barrett, *Langmuir*, 2003, **19**, 3297-3303.

30. M. Weijers, P. A. Barneveld, M. A. Cohen Stuart and R. W. Visschers, *Protein Science*, 2003, **12**, 2693-2703.
31. M. Müller, B. Kessler, N. Houbenov, K. Bohatá, Z. Pientka and E. Brynda, *Biomacromolecules*, 2006, **7**, 1285-1294.
32. P. Schwinté, V. Ball, B. Szalontai, Y. Haikel, J. C. Voegel and P. Schaaf, *Biomacromolecules*, 2002, **3**, 1135-1143.
33. G. Ladam, C. Gergely, B. Senger, G. Decher, J.-C. Voegel, P. Schaaf and F. J. G. Cuisinier, *Biomacromolecules*, 2000, **1**, 674-687.
34. F. Tristán, G. Palestino, J. L. Menchaca, E. Pérez, H. Atmani, F. Cuisinier and G. Ladam, *Biomacromolecules*, 2009, **10**, 2275-2283.
35. D. S. Salloum and J. B. Schlenoff, *Biomacromolecules*, 2004, **5**, 1089-1096.
36. S. Balamurugan, S. Mendez, S. S. Balamurugan, M. J. O'Brie and G. P. López, *Langmuir*, 2003, **19**, 2545-2549.
37. G. Ladam, P. Schaaf, F. J. G. Cuisinier, G. Decher and J.-C. Voegel, *Langmuir*, 2001, **17**, 878-882.
38. M. Rabe, D. Verdes and S. Seeger, *Advances in colloid and interface science*, 2011, **162**, 87-106.
39. C. J. F. Souza and E. E. Garcia-Rojas, *Food Hydrocolloids*, 2015, **47**, 124-129.
40. N. Kitabatake, A. Ishida and E. Doi, *Agricultural and Biological Chemistry*, 1988, **52**, 967-973.
41. R. Nakamura, Y. Takemori and S. Shitamori, *Agricultural and Biological Chemistry*, 1981, **45**, 1653-1659.
42. http://www.uniprot.org/uniprot/P01012).
43. A. Vidyasagar, C. Sung, K. Losensky and J. L. Lutkenhaus, *Macromolecules*, 2012, **45**, 9169-9176.
44. A. Quinn, E. Tjipto, A. Yu, T. R. Gengenbach and F. Caruso, *Langmuir*, 2007, **23**, 4944-4949.
45. J. D. Mendelsohn, S. Y. Yang, J. A. Hiller, A. I. Hochbaum and M. F. Rubner, *Biomacromolecules*, 2003, **4**, 96-106.
46. S. T. Dubas and J. B. Schlenoff, *Macromolecules*, 2001, **34**, 3736-3740.
47. J. J. Harris and M. L. Bruening, *Langmuir*, 2000, **16**, 2006-2013.
48. J. B. Schlenoff, *Langmuir*, 2014, **30**, 9625-9636.

**Graphical abstract**

1